NASA TM X-415

TECHNICAL MEMORANDUM

X-415

COMPARISON OF EXPERIMENTALLY OBTAINED PERFORMANCE OF TWO SINGLE-STAGE TURBINES WITH DESIGN RATIOS OF BLADE TO JET SPEED OF 0.191 AND 0.262 OPERATED IN HYDROGEN AND IN NITROGEN

By Robert Y. Wong and David L. Darmstadt

Lewis Research Center
Cleveland, Ohio

NATIONAL AERONAUTICS AND SPACE ADMINISTRATION

WASHINGTON

January 1961

NATIONAL AERONAUTICS AND SPACE ADMINISTRATION

TECHNICAL MEMORANDUM X-415

COMPARISON OF EXPERIMENTALLY OBTAINED PERFORMANCE OF TWO SINGLE-STAGE TURBINES WITH DESIGN RATIOS OF BLADE TO JET SPEED OF 0.191 AND 0.262 OPERATED IN HYDROGEN AND IN NITROGEN*

By Robert Y. Wong and David L. Darmstadt

SUMMARY

Two single-stage turbines were experimentally investigated over a range of blade- to jet-speed ratio in gaseous hydrogen and in gaseous nitrogen to determine the validity of using air criteria in the design of hydrogen turbines. Over the range of blade- to jet-speed ratio investigated, little difference in efficiency was obtained when each turbine was operated in each of the fluids. At design point the turbine designed for a blade- to jet-speed ratio of 0.191 had efficiencies of 0.430 and 0.418 in hydrogen and nitrogen, respectively. At design point, the turbine designed for a blade- to jet-speed ratio of 0.262 had an efficiency of 0.547 in these two fluids. The efficiencies of the turbines predicted theoretically using air criteria were found to agree closely in level with those obtained experimentally. This indicates the validity of using criteria based on air in the design and performance prediction of hydrogen turbines.

INTRODUCTION

In the field of auxiliary power turbines used on rockets and space vehicles, one of the most important factors to consider is the ability of the turbine to deliver high specific work output, because of the premium placed on the weight of fuel required to be carried aboard. One method of achieving this is to employ a high-energy fluid such as hydrogen to drive the turbine.

While there exists a great amount of information to guide the designer of a turbine to be run in air, very little is available for the hydrogen turbine. However, if it can be shown that design criteria for air turbines are applicable to hydrogen turbines, then the backlog of previous information can be utilized. Therefore, to explore this problem, an experimental investigation involving two single-stage turbines

*Title, Unclassified.

of the type suitable for hydrogen applications was undertaken. The turbines were designed for ratios of blade speed to jet speed of 0.191 and 0.262, which are considered to be within the range of current interest. The two turbines were tested in gaseous hydrogen and in gaseous nitrogen. Nitrogen was chosen because its thermodynamic properties are similar to those of air and because of its availability with a sufficiently low dewpoint. This report presents the results of this investigation and includes a comparison with theoretical performance based upon air criteria and the conventional Reynolds number exponent of -1/5.

SYMBOLS

A_{an} annulus area, sq ft

C loss coefficient (equal to $K(A/w)$ in ref. 3)

D_p pressure-surface diffusion parameter, $D_p = 1 - \left[\dfrac{\left(\frac{W}{W_{cr}}\right)_{p,min}}{\left(\frac{W}{W_{cr}}\right)_4}\right]$

D_s suction-surface diffusion parameter, $D_s = 1 - \left[\dfrac{\left(\frac{W}{W_{cr}}\right)_5}{\left(\frac{W}{W_{cr}}\right)_{s,max}}\right]$

d wheel diameter, in.

g gravitational constant, 32.17 ft/sec^2

Δh specific work output, Btu/lb

N rotational speed, rpm

p absolute pressure, lb/sq ft abs

R gas constant, ft-lb/(lb)($^\circ$R)

Re Reynolds number

r radius, in.

T absolute temperature, $^\circ$R

U	mean-section blade speed, ft/sec
V	absolute gas velocity, ft/sec
V_j	ideal gas velocity corresponding to total- to static-pressure ratio across turbine
W	relative gas velocity, ft/sec
w	weight-flow rate, lb/sec
α	absolute gas-flow angle measured from axial direction, deg
β	relative gas-flow angle measured from axial direction, deg
γ	ratio of specific heats
η_s	adiabatic efficiency based on total- to static-pressure ratio across turbine
ν	ratio of blade speed to jet speed, U/V_j
σ	solidity, ratio of blade chord to spacing

Subscripts:

b	base or reference value
cr	conditions at Mach 1.0
id	ideal
m	mean section
max	maximum
min	minimum
p	pressure surface
s	suction surface
sl	NASA standard sea-level conditions
x	axial direction
0	station at turbine inlet

2 station at stator outlet, just upstream of trailing edge

3 free-stream station between stator and rotor

4 station at rotor inlet, just downstream of leading edge

5 station at rotor outlet, just upstream of trailing edge

6 free-stream station at rotor outlet

7 station downstream of rotor in region of low velocity (see fig. 4)

Superscript:

' total or stagnation state

TURBINE DESIGN

Design Characteristics

The design characteristics selected for the subject turbines, hereafter referred to as turbines A and B, are presented in table I. From the table it is seen that turbines A and B have the same characteristics with respect to wheel size, blade height, weight flow, and wheel speed. They differ in pressure ratio and therefore in blade- to jet-speed ratio and work output.

Turbine A was the first-stage stator and unshrouded first-stage rotor investigated in reference 1. In this reference a design efficiency (based on total- to static-pressure ratio) of 0.51 was used. This efficiency was obtained from boundary-layer characteristics using experimentally obtained boundary-layer parameters. A theoretical efficiency of 0.548 for turbine B based on a total- to static-pressure ratio of 1.705 was obtained by the method of reference 2, which utilizes the velocity diagrams and an empirical loss coefficient. An empirical loss coefficient C_b was obtained from the experimental air data given in reference 2. This empirical loss coefficient was adjusted for the different velocity diagram and Reynolds number by the following equation, which is from reference 2:

$$C = C_b \left(\frac{\cot \alpha_{b,3}}{\cot \alpha_3}\right)\left(\frac{Re_b}{Re}\right)^{1/5}$$

where $C_b = 0.0216$, $\alpha_b = 60^\circ$, and $Re_b = 550{,}000$.

The Reynolds number for turbine B was computed using a mean of the average static-state conditions and relative velocity at the inlet and outlet of the stator and rotor. State conditions representative of proposed test conditions were selected for the computation (see EXPERIMENTAL PROCEDURE). The hydrogen case, which yielded the lowest Reynolds number (156,650) was chosen for use in the preceding equation for loss coefficient. This coefficient was then used in equations (19) and (20) of reference 3 to predict the design efficiency.

Velocity Diagrams

The design velocity diagrams for turbines A and B, including a sketch of the blading to indicate station nomenclature, are shown in table II. A detailed description of the design velocity-diagram construction for turbine A is presented in reference 1. The design velocity diagrams for turbine B were constructed for the free-stream stations 0, 3, and 6 at the mean blade radius to meet the design characteristics and the following additional assumptions:

(1) No radial flow variations

(2) Equal rotor inlet and outlet relative tangential velocities

(3) A 1/3 and 2/3 split in total-pressure loss between the stator and rotor, respectively

From table II it can be seen that design free-stream turning in the stators is 80.0° and 79.9° for turbines A and B, respectively, and design free-stream turning in the rotors is 152.0° and 147.8°, respectively. Also, from table II, it is seen that stator A is choked and stator B is unchoked. Turbines A and B were designed with 69.1° and 58.1° exit whirl, respectively.

The velocities at stations 2, 4, and 5 for turbine B were computed from the adjacent free-stream diagrams. These velocities were used in the blade design and are based on the following assumptions:

(1) No change in tangential component of velocity

(2) Continuity, no loss in total pressure, and trailing-edge blockage of 23.7 percent for the stator and 10.4 percent for the rotor.

Stator Design

The stator design for turbine A is presented in reference 1. Turbine B was designed to pass the same weight flow. The blade profile and

number of baldes for the two turbines are the same, but the blades are oriented with a free-stream stator outlet angle of 79.9° for turbine B and 80.0° for turbine A. The throat dimensions are 0.049 and 0.051 inch for turbines A and B, respectively. It should be noted that, since turbine B is unchoked, it required a larger throat area, and thus the small differences in angle and throat dimension between the turbines are the result of the different flow coefficients that were assumed in the design. The flow coefficients assumed were 0.911 and 0.955 for turbines A and B, respectively. Each stator had 110 blades and a solidity σ of 1.8. Stator blade coordinates are given in table III.

Rotor Design

The rotor design for turbine A is discussed in reference 1. The rotor blade profile for turbine B was obtained at the mean radius from consideration of velocity diffusion limits on the suction and pressure surfaces. These limits include a minimum suction-surface diffusion with a total diffusion limited to on the order of 0.5 (ref. 4). The velocity distribution obtained in the final design is presented in figure 1. It can be seen that the blade was designed for a minimum diffusion on the suction surface D_s. The total diffusion ($D_{tot} = D_s + D_p$) was computed to be 0.43. The solidity of the rotor was 2.00. Since the hub to tip radius ratio is 0.945, radial flow variations were ignored. Rotor blade coordinates for both turbines are given in table IV; the blade profiles for both turbines are shown in figure 2; and photographs of the rotors for both turbines are shown in figure 3. A tip clearance of 0.013 inch was used for both rotors.

APPARATUS AND INSTRUMENTATION

The apparatus used in the investigation consisted of the housing in which turbines A and B were installed, as well as suitable piping and controls to provide uniform inlet flow to the turbine and an exhaust to atmosphere. A dynamometer cradled with a speed-reducing gearbox and connected to the turbine was used to absorb the power. A diagrammatic sketch of the rig is presented in figure 4.

The torque imparted to the dynamometer was measured by a strain-gage load cell. Turbine bearing and seal losses were obtained by motoring the turbine with the rotor removed. These losses were found to vary nonlinearly with speed and were added to measured shaft power to obtain blade power.

Weight flow was measured by a calibrated sharp-edged orifice installed according to ASME Power Test Codes. Turbine speed was measured by an electronic tachometer in conjunction with a magnetic pickup and a 200-tooth sprocket gear mounted on the dynamometer shaft. All pressures

were measured with static taps connected to strain-gage pressure transducers. Four static taps oriented 90° apart were manifolded together and placed at both the hub and tip at stations 0, 3, and 6. The readings of the manifolded taps at the hub and tip were then averaged at each station for purposes of computation. In order to obtain maximum accuracy, small-capacity transducers were used to measure differential pressures between measuring stations, and a highly accurate pressure transducer was then selected for the reference pressure.

Temperature measurements at the inlet of the turbine were measured with bare-wire spike thermocouples. A shielded thermocouple rake was installed at station 7 (see fig. 4) to minimize the effect of flow angle on the indicated exit temperature. All pressure and temperature data were recorded on magnetic tape with an automatic voltage digitizer and processed in an electronic computer.

EXPERIMENTAL PROCEDURE

The experimental investigation was conducted by operating turbine A in nitrogen and in hydrogen at inlet pressures of 90 and 65 pounds per square inch absolute, respectively. The pressure level at which each turbine was run was selected from consideration of pressure ratio, running time, torque level, and instrumentation limitations. Outlet pressure was varied to give pressure ratios of from 2.03 to 3.58. Turbine inlet temperature, although constantly dropping because of the flow work done in the gas supply vessel, averaged approximately 38° F for nitrogen and 62° F for hydrogen.

Turbine B was operated in nitrogen and in hydrogen at inlet pressures of 90 and 74 pounds per square inch absolute, respectively. Outlet pressure was varied to give pressure ratios of from 1.50 to 3.74. Average turbine inlet temperature was 20° F for nitrogen and 70° F for hydrogen. With nitrogen as the working fluid, turbine speed was varied from about 50 to 150 percent of design speed (approx. 5600 rpm) in increments of 200 to 250 rpm. For hydrogen runs, the turbine speed was varied from 15 to 100 percent of design speed (approx. 22,000 rpm) in increments of 1000 rpm.

CALCULATIONS

The turbine was rated on the basis of the ratio of inlet total pressure to outlet static pressure. The inlet total pressure p'_0 was calculated from weight flow, inlet static pressure, and inlet total temperatures from the following equation, which is from reference 2:

$$\frac{w\sqrt{T'}}{pA_{an}} = \left[\frac{2\gamma g}{(\gamma - 1)R}\right]^{-1/2} \left\{\left[\left(\frac{p'}{p}\right)^{\frac{\gamma-1}{\gamma}} - 1\right] + \left[\left(\frac{p'}{p}\right)^{\frac{\gamma-1}{\gamma}} - 1\right]^2\right\}^{1/2}$$

Actual turbine power was based on product of rotor speed and sum of shaft and friction torque. Turbine efficiency was calculated as the ratio of actual turbine power to ideal power, which was obtained from weight flow, inlet total temperature, overall turbine total- to static-pressure ratio, and real gas temperature-pressure-entropy data supplied in reference 5.

RESULTS AND DISCUSSION

Specific Work

The performance of turbine A is presented in figure 5, where specific work output $\Delta h'$ is plotted against rotational speed N in each fluid corrected to standard temperature (518.7° R). With turbine A operating in hydrogen at design speed (20,940 rpm) and design pressure ratio (2.94), the work output is approximately 200 Btu per pound (fig. 5(a)). This is below design work output of 240.71 Btu per pound. With turbine A operating in nitrogen at design speed (5617 rpm) and design pressure ratio (2.94), the work output is approximately 14.1 Btu per pound by interpolation (fig. 5(b)). This is also below design work output of 17.48 Btu per pound. These results are comparable to those presented in reference 1.

The performance of turbine B is presented in figure 6. With turbine B operating in hydrogen at design speed (20,940 rpm) and design pressure ratio (1.705), the work output is approximately 136 Btu per pound by interpolation (fig. 6(a)). This agrees well with design work output of 137.73 Btu per pound. With turbine B operating in nitrogen at design speed (5617 rpm) and design pressure ratio (1.705), the work output is 9.94 Btu per pound (fig. 6(b)), which also agrees well with design work output of 9.95 Btu per pound.

Efficiency and Blade- to Jet-Speed Ratio

The variation of static efficiency with blade- to jet-speed ratio for turbine A operating in hydrogen and in nitrogen at nominally design pressure ratio is shown in figure 7(a). Over the range of blade- to jet-speed ratio investigated, very little difference in efficiency was obtained when the turbine was operated in the two fluids. Further, at

design blade- to jet-speed ratio (0.191) the static efficiency in hydrogen is 0.430 and in nitrogen it is 0.418. Figure 7(b) shows the variation in static efficiency with blade- to jet-speed ratio for turbine A operating at all pressure ratios (see fig. 5) in hydrogen and in nitrogen. Substantially the same results were obtained at all pressure ratios as were obtained at design pressure ratio only. From figure 7 it is seen that, within experimental accuracy, no significant fluid effect has been demonstrated.

Figure 8(a) presents the variation of static efficiency with blade- to jet-speed ratio for turbine B operating at nominally design pressure ratio in both hydrogen and nitrogen. The complete lack of fluid effect can be noted over the range investigated. Further, the static efficiency is 0.547 at design blade- to jet-speed ratio of 0.262. Figure 8(b) presents the variation in static efficiency with blade- to jet-speed ratio for turbine B operating at all pressure ratios (see fig. 6) in hydrogen and nitrogen. Again, substantially the same results were obtained at all pressure ratios as were obtained at design pressure ratio only.

Pressure Distribution

The pressure distribution through turbines A and B is presented in figures 9(a) and (b), respectively. Figure 9(a) shows that, for turbine A at design overall pressure ratio, stator exit design static pressure was not achieved. This indicates a small mismatch between the rotor and stator throat areas, so that design stator exit velocity diagram could not be achieved at design overall pressure ratio. Figure 9(b) shows that, for turbine B at near-design pressure ratio (both below and above), the stator exit static pressure is less than that designed. This again indicates a small mismatch between stator and rotor areas. For turbine B, however, the mismatch is such that slightly higher than design stator exit velocity was obtained.

Weight-Flow Characteristics

From a study of the weight flow passed by both turbines operating nominally at design overall pressure ratio and design speed, it was found that the weight flow was 10.5 ± 0.6 percent greater than design for both hydrogen and nitrogen. Measurement of the stator throat area of turbine A indicated that the throat area was made 8.5 percent too large. This, coupled with the high stator loss assumption, accounts for the excessive measured weight flow. The flow coefficient (defined as ratio of actual weight flow to ideal weight flow) was 0.922 for hydrogen and 0.928 for nitrogen.

A check of the throat area of turbine B revealed that it was made 5.6 percent larger than designed for. Since the stator of this turbine was not designed to choke, overexpansion of the stator as indicated by figure 9(b) will also result in a high weight flow. For the nitrogen case, using figure 9(b), the overexpansion at design point was computed to result in a 4.4 percent higher flow, which again accounts for the excessive measured flow. The flow coefficient for the stator of turbine B was found to be 0.971 for hydrogen and 0.963 for nitrogen. The difference in level of flow coefficient between the two turbines may be attributable to the difference in average flow velocity through the nozzle and experimental error. The point to be noted is that for each turbine the flow coefficient did not vary significantly with the driving fluid used.

Comparison of Experimental Results with Theory

Theoretical efficiencies for turbines A and B were computed by the method outlined under TURBINE DESIGN. Briefly, this method involves using an empirical loss coefficient (obtained from air testing) that is adjusted for Reynolds number to the 1/5 power and for design velocity diagram to obtain a theoretical efficiency.

For turbine A operating at nominal test conditions in hydrogen and in nitrogen at design pressure ratio and design speed, the Reynolds numbers (based on blade height) were computed to be 190,020 and 532,860, respectively. The Reynolds numbers were used to compute theoretical efficiencies, which were 0.441 and 0.462 for hydrogen and nitrogen, respectively. The experimental efficiencies of 0.430 for hydrogen and 0.418 for nitrogen agree well with the predicted levels.

For turbine B operating at nominal test conditions in hydrogen and in nitrogen at design pressure ratio and design speed, the Reynolds numbers were computed to be 156,650 and 405,608, respectively. Corresponding theoretical efficiencies of 0.548 and 0.572 were computed. The experimentally obtained efficiency of 0.547 for both fluids agrees well with the predicted level.

The agreement in level between the theoretical and experimental efficiencies shown here demonstrates the validity of using air criteria in the design and performance prediction of turbines to be operated in hydrogen.

SUMMARY OF RESULTS

Two single-stage turbines were experimentally investigated over a range of blade- to jet-speed ratios in gaseous hydrogen and in gaseous

nitrogen to determine the validity of using air criteria in the design of hydrogen turbines. The following summarizes the results obtained:

1. Over the range of blade- to jet-speed ratio investigated, little effect on efficiency was obtained when each turbine was operated in hydrogen and in nitrogen.

2. At design point, the turbine designed for a blade- to jet-speed ratio of 0.191 had efficiencies of 0.430 and 0.418 in hydrogen and nitrogen, respectively.

3. At design point, the turbine designed for a blade- to jet-speed ratio of 0.262 had an efficiency of 0.547 in both nitrogen and hydrogen.

4. The efficiencies of the turbines predicted theoretically using air criteria were found to agree closely in level with those obtained experimentally. This indicates the validity of using criteria based on air in the design and performance prediction of hydrogen turbines.

Lewis Research Center
National Aeronautics and Space Administration
Cleveland, Ohio, August 26, 1960

REFERENCES

1. Kofskey, Milton G.: Performance Evaluation of a Two-Stage Turbine Designed for a Ratio of Blade Speed to Jet Speed of 0.146. NASA TM X-146, 1959.

2. Wong, Robert Y., and Monroe, Daniel E.: Investigation of a 4.5-Inch-Mean-Diameter Two-Stage Axial-Flow Turbine Suitable for Auxiliary Power Drives. NASA MEMO 4-6-59E, 1959.

3. Stewart, Warner L.: Analytical Investigation of Multistage-Turbine Efficiency Characteristics in Terms of Work and Speed Requirements. NACA RM E57K22b, 1958.

4. Stewart, Warner L., Whitney, Warren J., and Miser, James W.: Use of Effective Momentum Thickness in Describing Turbine Rotor-Blade Losses. NACA RM E56B29, 1956.

5. Hilsenrath, Joseph, et al.: Tables of Thermal Properties of Gases. Cir. 564, NBS, Nov. 1, 1955.

TABLE I. - TURBINE DESIGN CHARACTERISTICS AT STANDARD TEMPERATURE AND PRESSURE (T_{sl} = 518.7° R; p_{sl} = 2116 lb/sq ft abs)

Turbine	A	B
Blade- to jet-speed ratio, ν	0.191	0.262
Total- to static-pressure ratio, p'_0/p_6	2.940	1.705
Static efficiency, η_s	0.510	0.548
Ideal hydrogen specific work, $\Delta h'_{id}$, Btu/lb Ideal nitrogen specific work, $\Delta h'_{id}$, Btu/lb	471.98 34.29	251.34 18.13
Hydrogen specific work, $\Delta h'$, Btu/lb Nitrogen specific work, $\Delta h'$, Btu/lb	240.71 17.48	137.73 9.94
Hydrogen weight flow, w, lb/sec Nitrogen weight flow, w, lb/sec	0.1269 .475	0.1269 .475
Ratio of blade mean-section speed to critical velocity, $(U/V_{cr})_3$	0.241	0.241
Rotational speed in hydrogen, N, rpm Rotational speed in nitrogen, N, rpm	20,940 5,617	20,940 5,617
Mean wheel diameter, d_m, in.	10.2	10.2
Blade height, in.	0.286	0.286

TABLE II. - VELOCITY DIAGRAMS

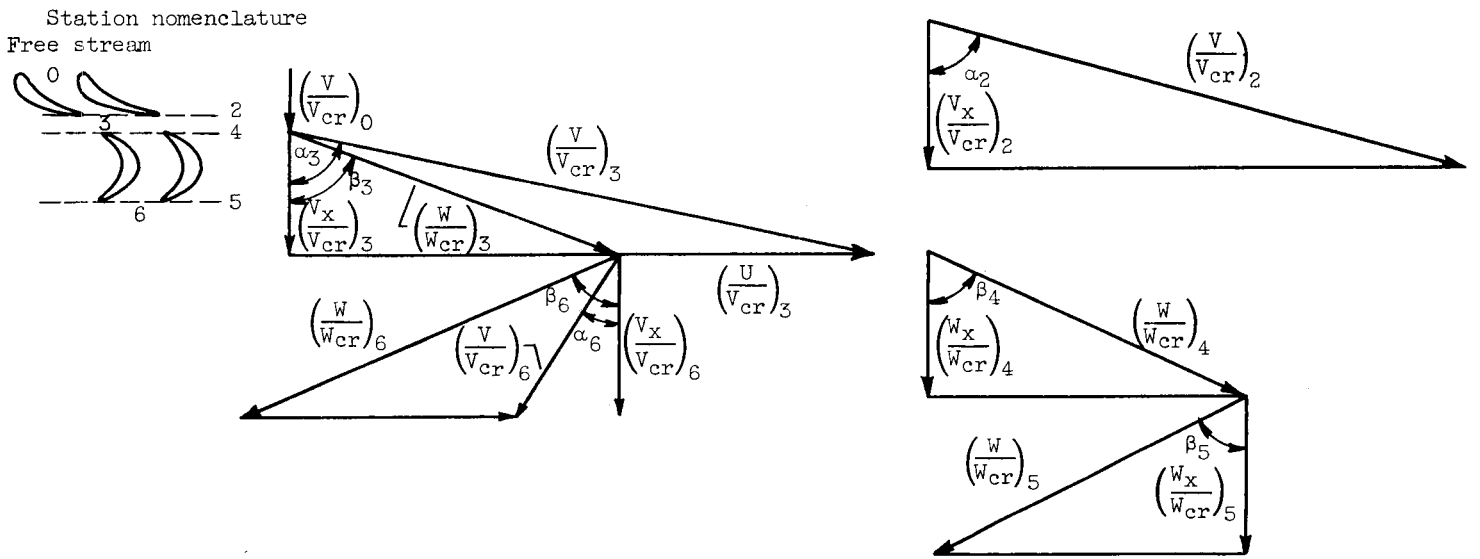

Turbine	$\left(\frac{V}{V_{cr}}\right)_0$	$\left(\frac{V}{V_{cr}}\right)_2$	$\left(\frac{V_x}{V_{cr}}\right)_2$	α_2	$\left(\frac{V}{V_{cr}}\right)_3$	$\left(\frac{V_x}{V_{cr}}\right)_3$	$\left(\frac{U}{V_{cr}}\right)_3$	$\left(\frac{W}{W_{cr}}\right)_3$	α_3	β_3	$\left(\frac{W}{W_{cr}}\right)_4$	$\left(\frac{W_x}{W_{cr}}\right)_4$	β_4
A	0.098	1.175	0.228	76°30'	1.095	0.190	0.241	0.894	80°	77°12'	0.939	0.232	75°42'
B	0.097	0.743	0.172	76°37'	0.734	0.129	0.241	0.512	79°53'	75°1'	0.516	0.150	73°9'

Turbine	$\left(\frac{W}{W_{cr}}\right)_5$	$\left(\frac{W_x}{W_{cr}}\right)_5$	β_5	$\left(\frac{W}{W_{cr}}\right)_6$	$\left(\frac{V}{V_{cr}}\right)_6$	$\left(\frac{V_x}{V_{cr}}\right)_6$	β_6	α_6	$\left(\frac{U}{V_{cr}}\right)_6$
A	0.930	0.320	69°50'	0.904	0.687	0.245	74°47'	69°05'	0.259
B	0.523	0.173	70°41'	0.518	0.296	0.156	72°41'	58°08'	0.251

TABLE III. - STATOR BLADE COORDINATES

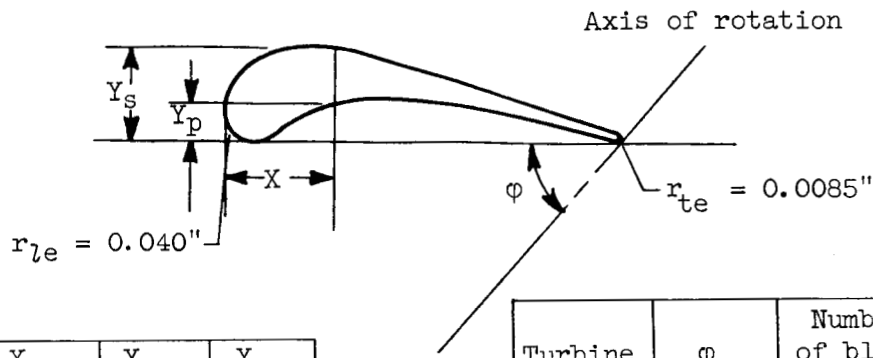

X, in.	Y_p, in.	Y_s, in.
0	0.040	0.040
.050	.001	.112
.100	.026	.129
.150	.044	.128
.200	.054	.115
.250	.056	.100
.300	.051	.085
.350	.042	.070
.400	.030	.054
.450	.018	.038
.500	.004	.023
.523	.008	.008

Turbine	φ	Number of blades
A	59°10'	110
B	59°05'	110

TABLE IV. - ROTOR BLADE COORDINATES FOR MEAN SECTION

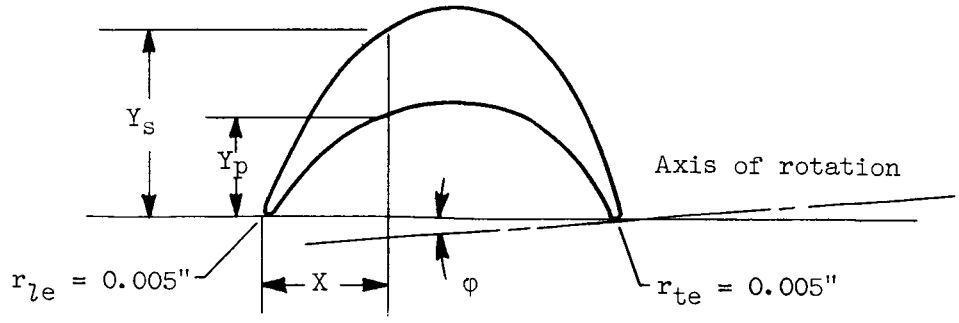

X, in.	Turbine A ($\varphi = 8^{\circ}20'$; 110 blades)		Turbine B ($\varphi = 5^{\circ}10'$; 110 blades)	
	Y_p, in.	Y_s, in.	Y_p, in.	Y_s, in.
0.0000	0.0050	0.0050	0.0050	0.0050
.0100	.0000	.0665	.0524	.0052
.0250	.0465	.2444	.1225	.0544
.0500	.0944	.3180	.2407	.1440
.0750	.1276	.3577	.3396	.1818
.1000	.1531	.3844	.3895	.2089
.1250	.1727	.4037	.4210	.2285
.1500	.1882	.4176	.4416	.2440
.1750	.2003	.4276	.4552	.2550
.2000	.2095	.4338	.4634	.2631
.2250	.2158	.4368	.4673	.2676
.2500	.2194	.4362	.4675	.2701
.2750	.2209	.4321	.4639	.2705
.3000	.2196	.4246	.4567	.2683
.3250	.2161	.4137	.4457	.2636
.3500	.2105	.3990	.4298	.2562
.3750	.2022	.3796	.4086	.2457
.4000	.1910	.3530	.3817	.2325
.4250	.1769	.3162	.3467	.2165
.4500	.1596	.2685	.3005	.1951
.4750	.1378	↑	.2467	.1710
.5000	.1114	Straight	.1904	.1419
.5250	.0782	line	.1348	.1038
.5500	.0357		.0797	.0544
.5715	.0000		------	------
.5750	------	↓	.0244	.0009
.5765	.0050	.0050	------	------
.5818	------	------	------	------
.5836	------	------	.0050	.0050

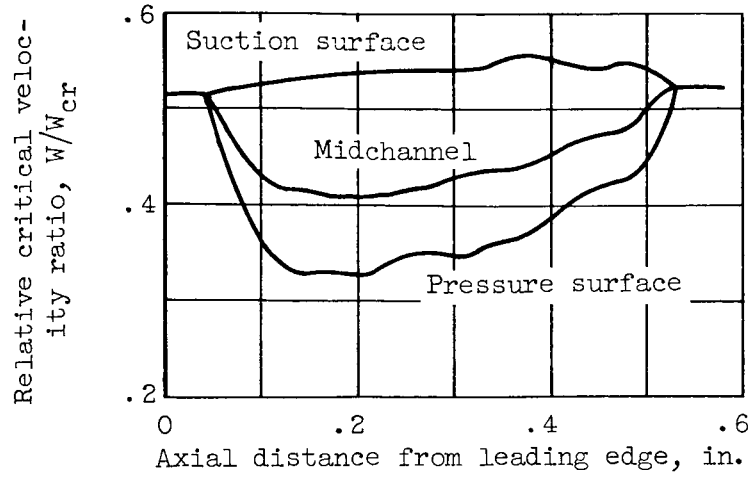

Figure 1. - Rotor channel velocity distribution through turbine B.

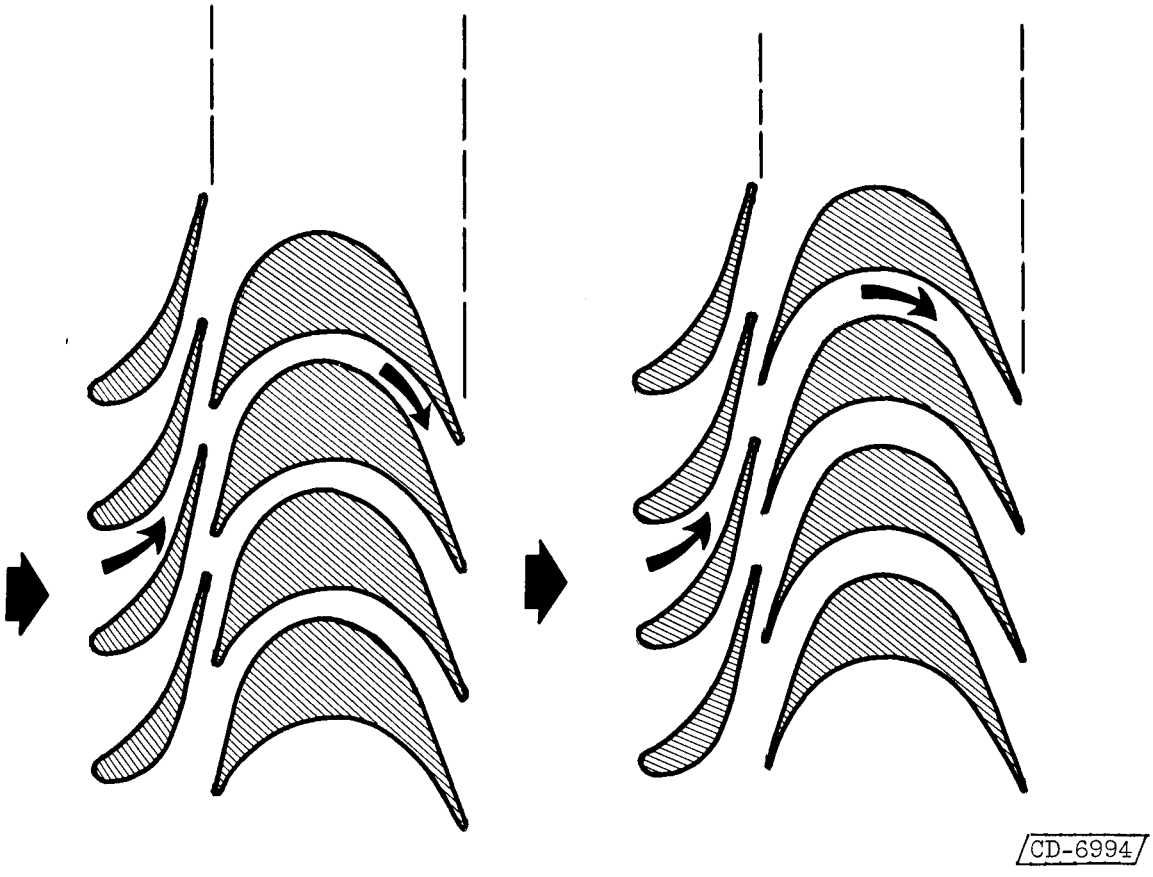

Figure 2. - Sketch of turbine blading.

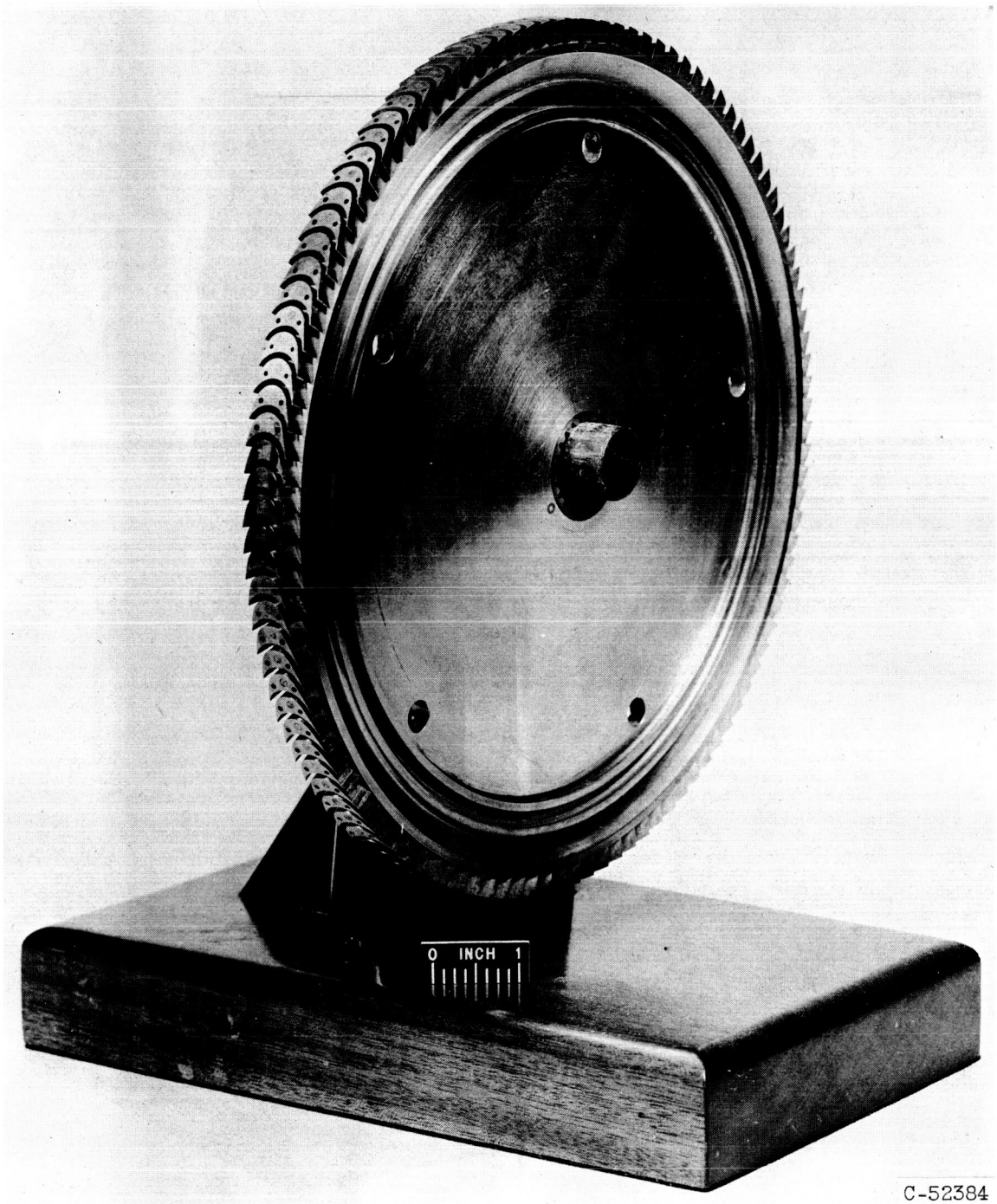

(a) Turbine A.

Figure 3. - Photographs of rotors.

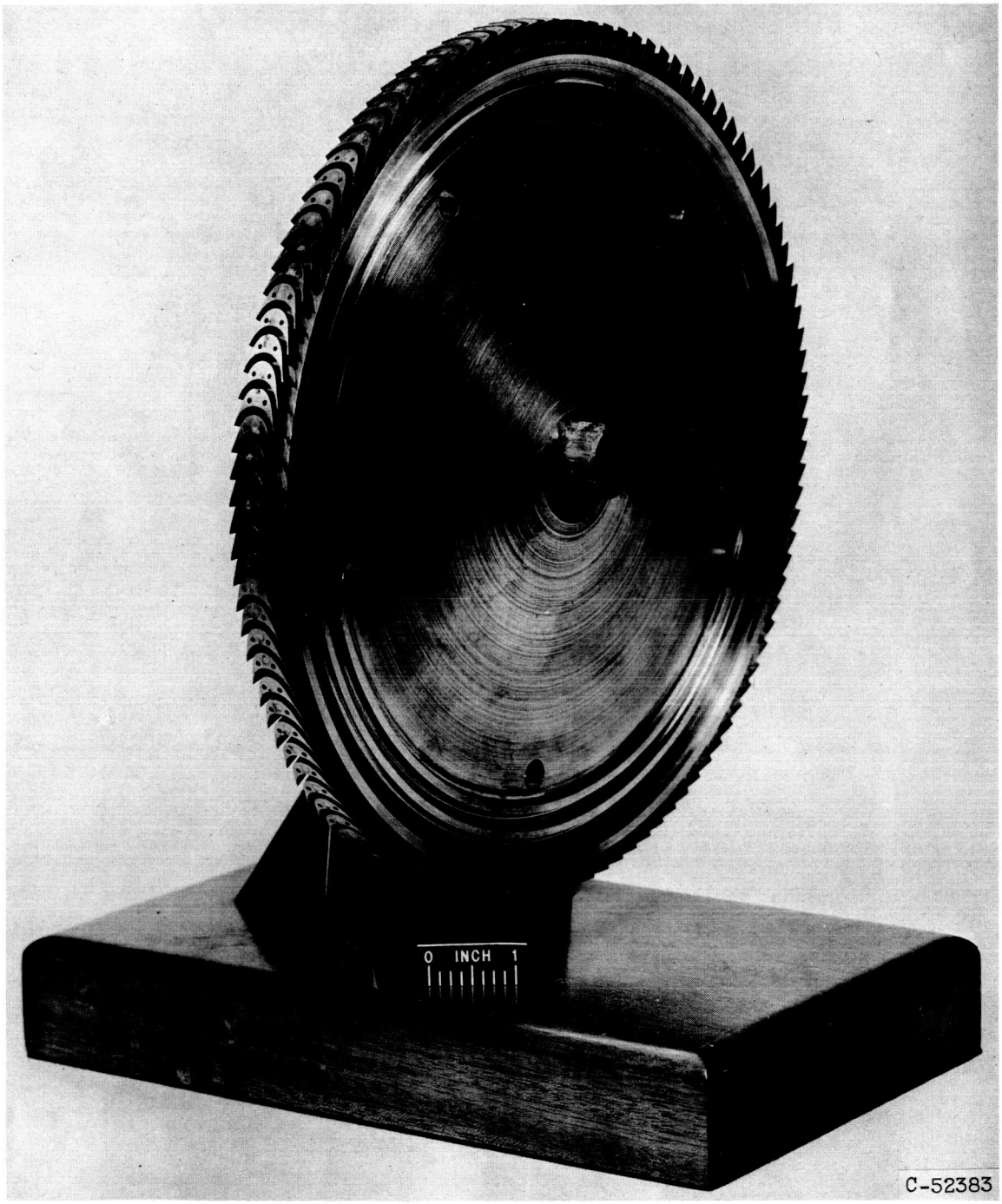

(b) Turbine B.

Figure 3. - Concluded. Photographs of rotors.

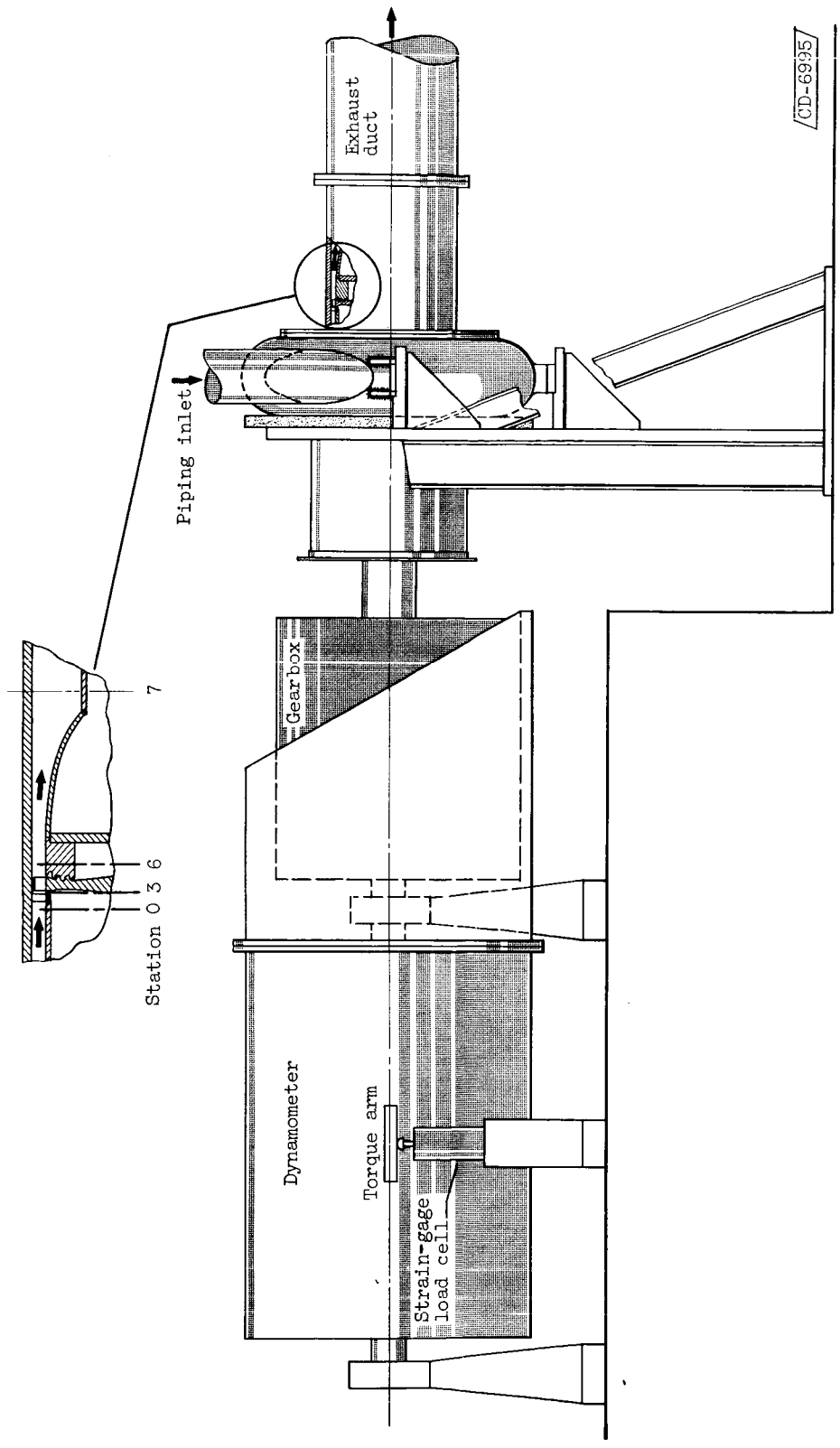

Figure 4. - Sketch of test apparatus.

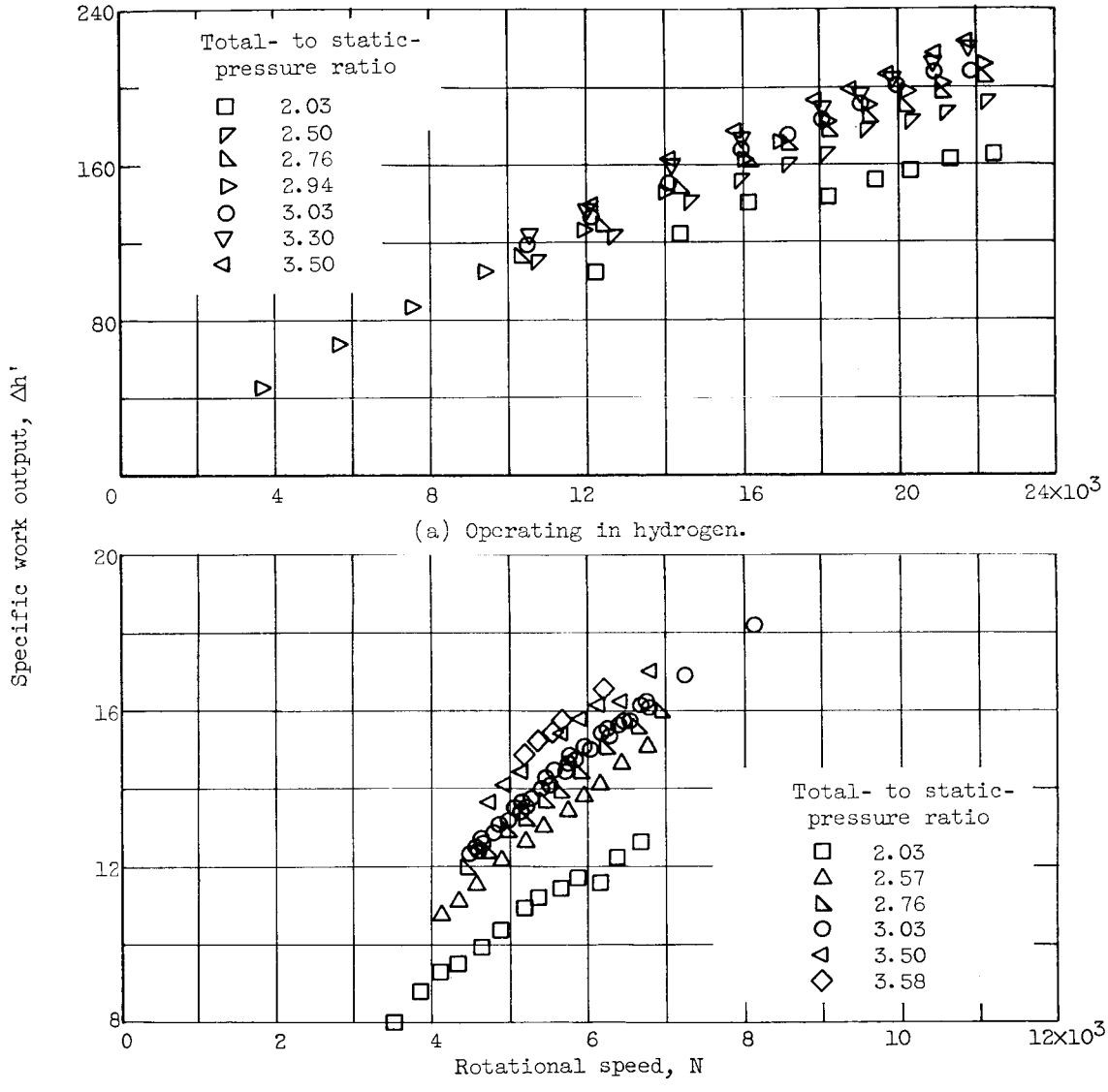

(a) Operating in hydrogen.

(b) Operating in nitrogen.

Figure 5. - Experimentally obtained performance of turbine A.

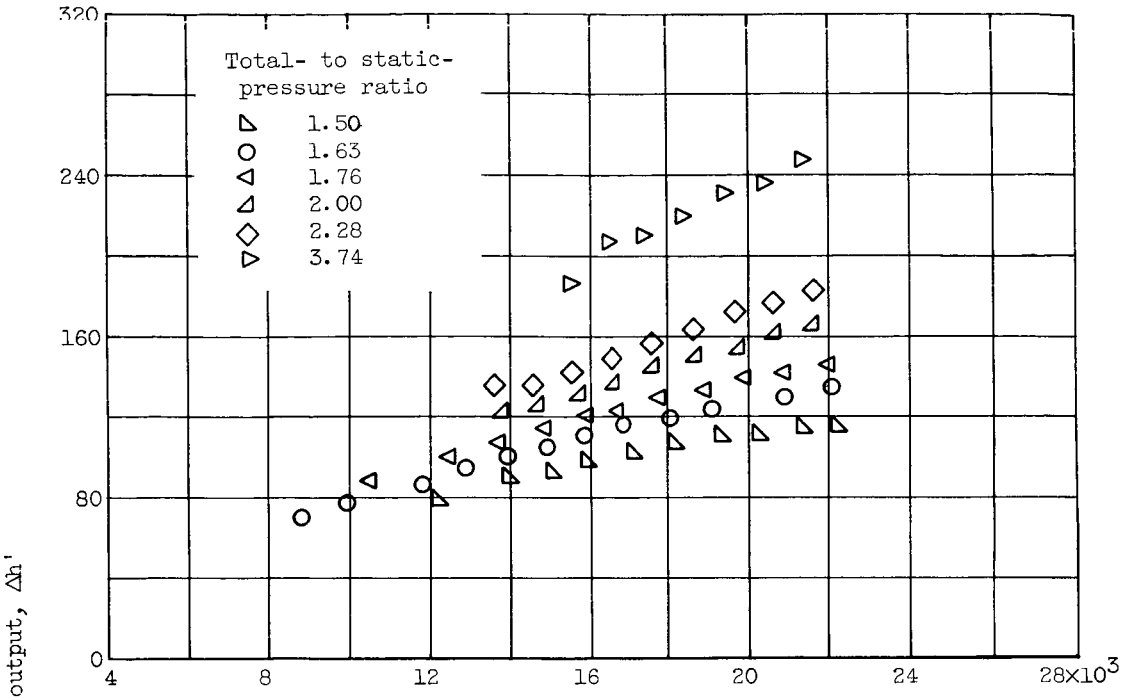

(a) Operating in hydrogen.

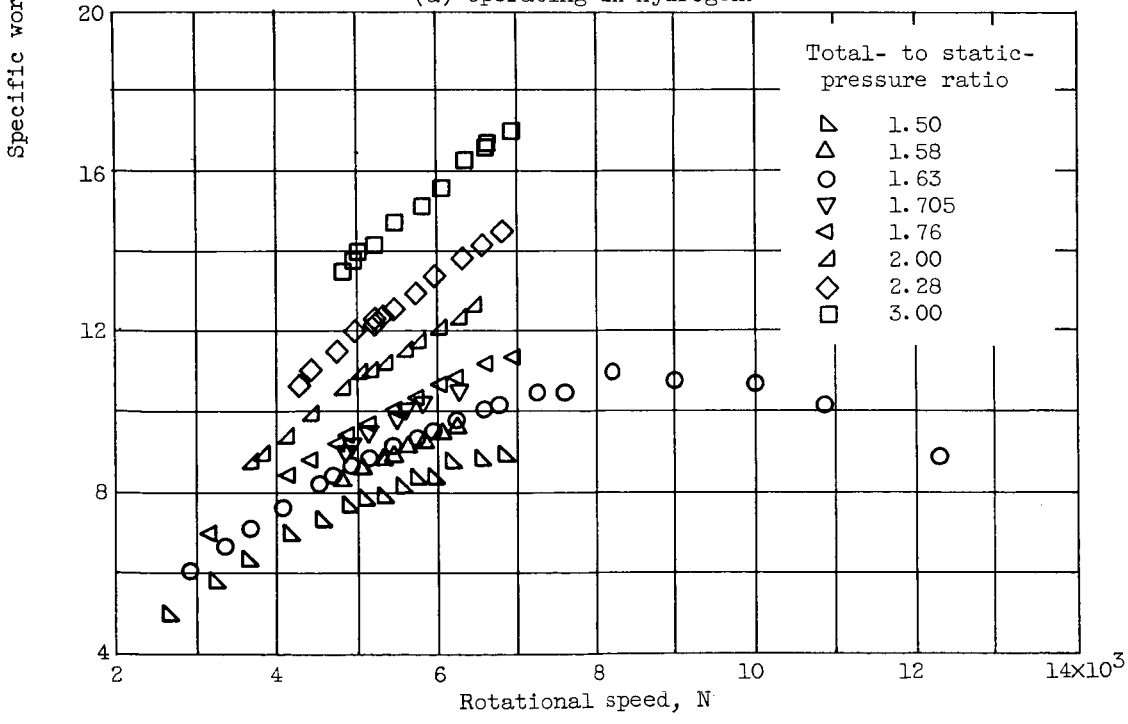

(b) Operating in nitrogen.

Figure 6. - Experimentally obtained performance of turbine B.

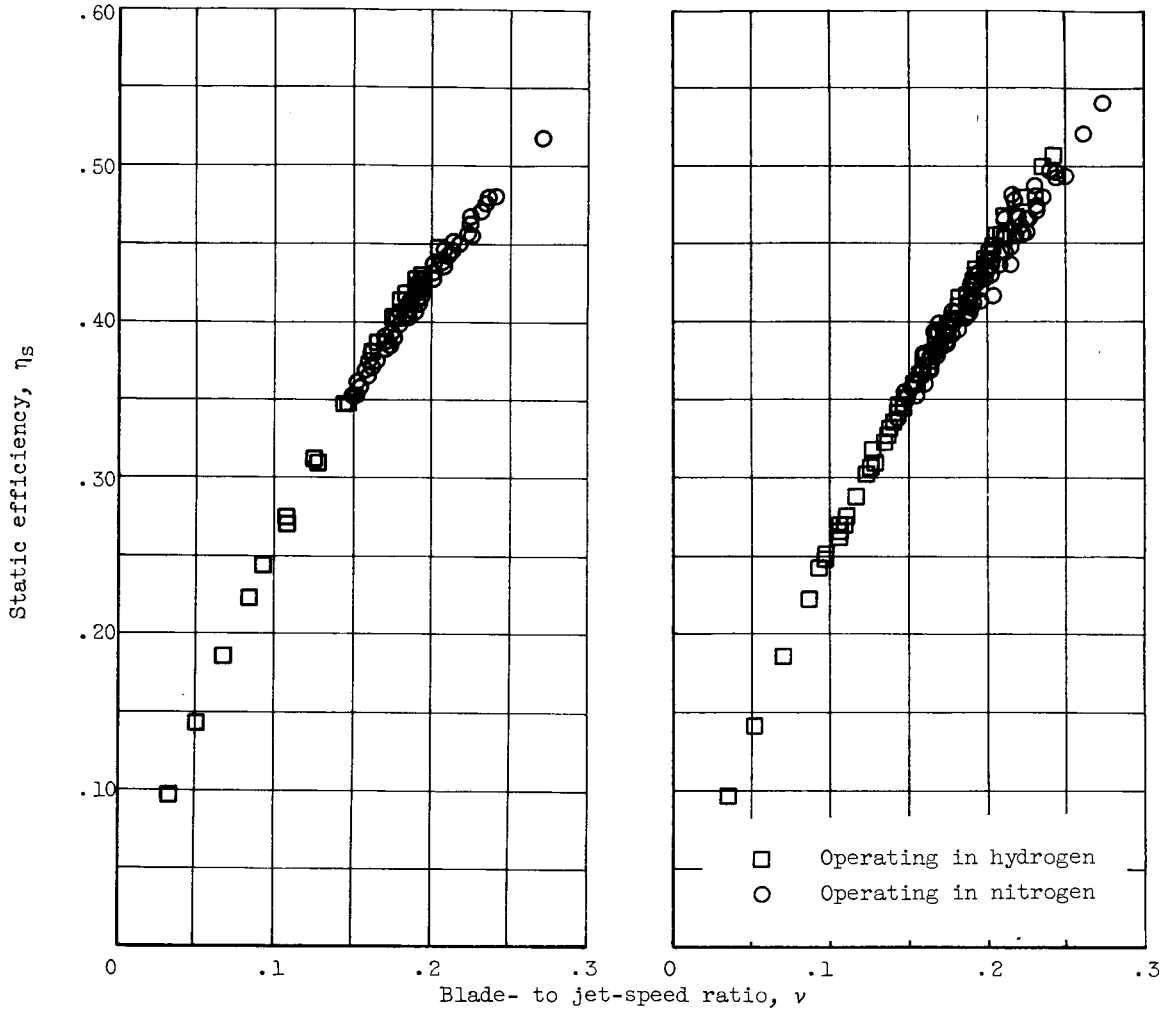

(a) Nominal design pressure ratio. (b) All pressure ratios.

Figure 7. - Experimentally obtained variation of efficiency with blade- to jet-speed ratio for turbine A operating in hydrogen and in nitrogen.

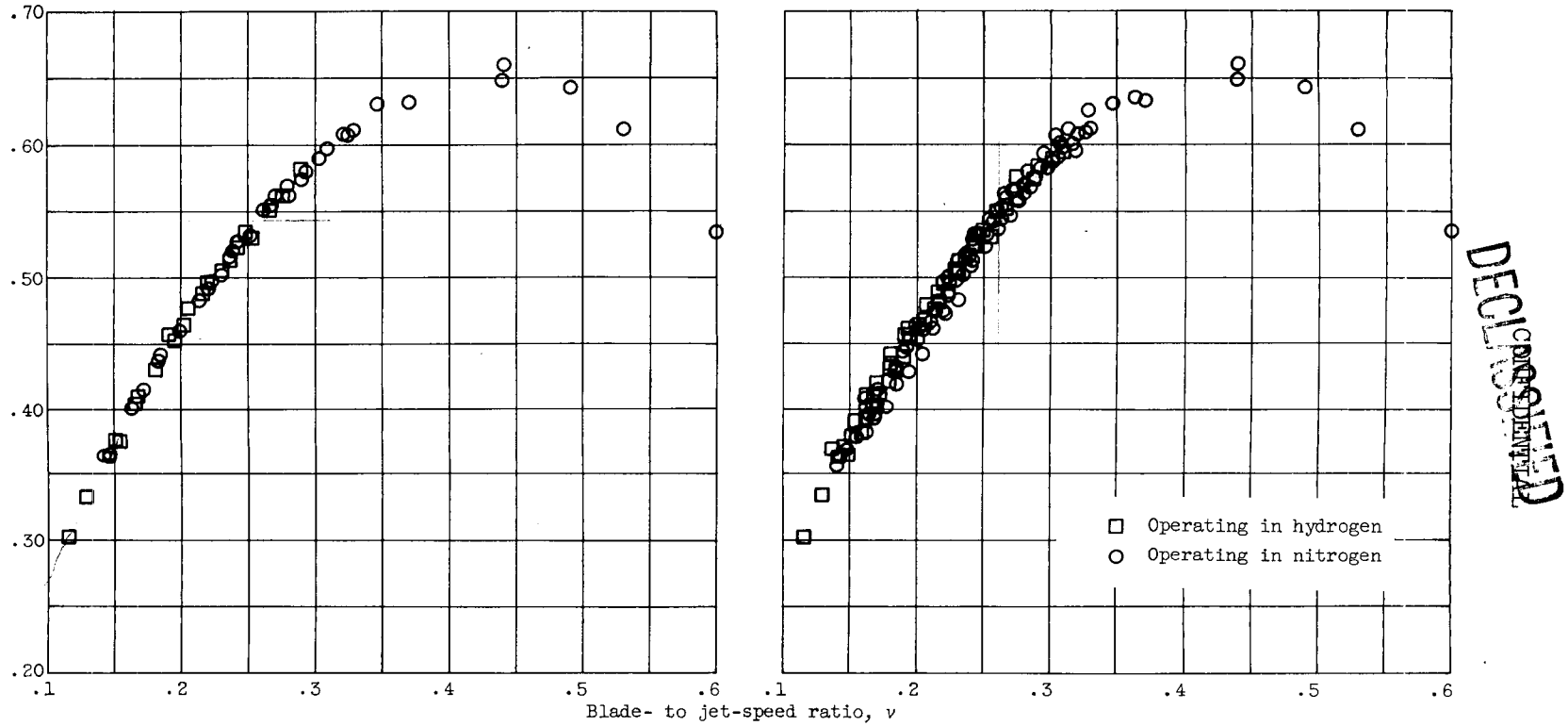

(a) Nominal design pressure ratio.

(b) All pressure ratios.

Figure 8. - Experimentally obtained variation of efficiency with blade- to jet-speed ratio for turbine B operating in hydrogen and in nitrogen.

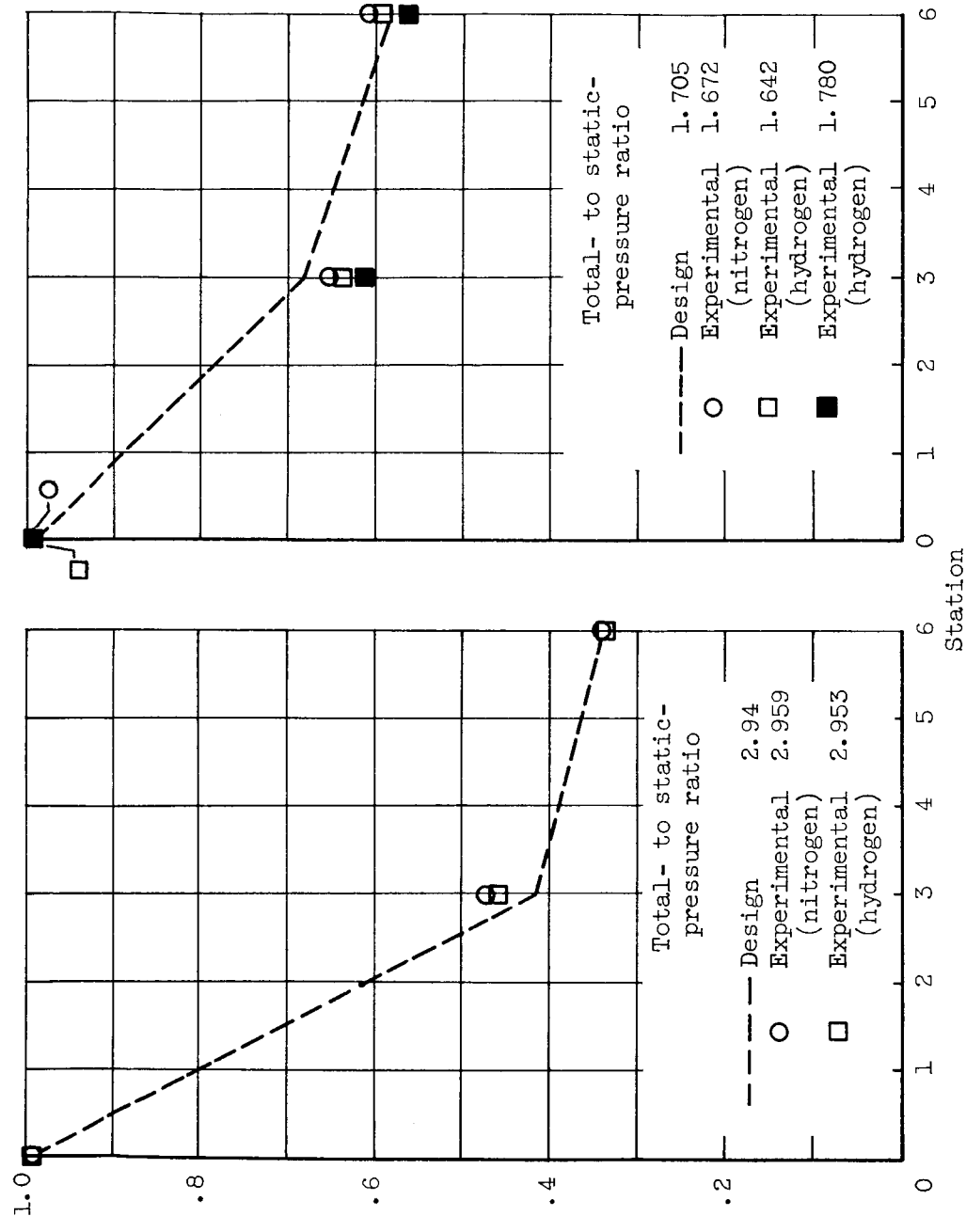

(a) Turbine A.

(b) Turbine B.

Figure 9. - Static-pressure distribution.